Affino-Proteomic Analysis of Bumped Kinase Inhibitor BKI-1708 in *Toxoplasma gondii* and Human Fibroblast Host Cells

Maria Cristina Ferreira de Sousa *, Joachim Müller, Manfred Heller, Anne-Christine Uldry, Sophie Braga-Lagache, Kayode K. Ojo, Wesley C. Van Voorhis, Andrew Hemphill *

Posted Date: 15 April 2026

doi: 10.20944/preprints202604.0997.v1

Keywords: *Toxoplasma gondii*; drug treatment; bumped kinase inhibitors; affinity chromatography; proteomics; drug targets

 doi:10.20944/preprints202604.0997.v1

Article

Affino-Proteomic Analysis of Bumped Kinase Inhibitor BKI-1708 in *Toxoplasma gondii* and Human Fibroblast Host Cells

Maria Cristina Ferreira de Sousa [1,2,*], Joachim Müller [1], Manfred Heller [3], Anne-Christine Uldry [3], Sophie Braga-Lagache [3], Kayode K. Ojo [4], Wesley C. Van Voorhis [4] and Andrew Hemphill [1,*]

[1] Institute of Parasitology, Vetsuisse Faculty, University of Bern, Switzerland

[2] Graduate School for Cellular and Biomedical Sciences (GCB), University of Bern, Switzerland

[3] Proteomics and Mass Spectrometry Core Facility, Department for BioMedical Research (DBMR), University of Bern, Switzerland

[4] Department of Medicine, Center for Emerging and Re-Emerging Infectious Diseases, University of Washington, Seattle, WA 98109-4766, USA

* Correspondence: maria.ferreira@unibe.ch (M.F.); andrew.hemphill@unibe.ch (A.H.)

Abstract

Bumped kinase inhibitor 1708 (BKI-1708), previously demonstrated to target apicomplexan kinases and CDPK1 and MAPKL1, exhibits remarkable activity against *Toxoplasma gondii* infection both *in vitro* and *in vivo*. Notably, BKI-1708 does not affect the viability of mammalian cells. Upon exposure to BKI-1708 exposure, *T. gondii* tachyzoites form large multinucleated complexes named baryzoites and remain trapped in within host cells. In this study, additional potential molecular targets for BKI-1708 were identified in soluble extracts of *T. gondii* ME49 tachyzoites and human foreskin fibroblasts (HFF) using differential affinity chromatography coupled to mass spectrometry (DAC-MS). Beyond kinases, secondary interactions in *T. gondii* involved the binding of proteins associated with cell division, cytoskeleton, vesicular trafficking, secretory organelles, and transcriptional and translational regulators. In non-infected HFFs, BKI-1708 interactors included cytoskeletal regulators along with multiple RNA/DNA-binding proteins. Upon infection, this profile shifted, with cytoskeletal components no longer detected, while nucleic acid–binding proteins remained present, consistent with infection-induced chromatin and transcriptional remodeling. This multi-target interference could contribute to the impaired cytokinesis and the formation of multinucleated baryzoites, aligning with the concept that antiprotozoal drugs exert efficacy through coordinated perturbation of multiple cellular processes rather than a single dominant target.

Keywords: *Toxoplasma gondii*; drug treatment; bumped kinase inhibitors; affinity chromatography; proteomics; drug targets

1. Introduction

Toxoplasma gondii is an obligate intracellular apicomplexan parasite of significant medical and veterinary importance, being the causative agent of the globally prevalent zoonosis toxoplasmosis [1]. Its life cycle is facultatively heteroxenous, with sexual reproduction confined to felids, and gamogony and oocyst formation taking place in the intestinal epithelium [2]. Numerous intermediate hosts, particularly man and small ruminants, acquire infection tby consuming sporulated oocysts from contaminated food or water, or via undercooked meat harbouring tissue cysts [1,3,4]. After invasion of enterocytes in the small intestine, parasites differentiate into rapidly-replicating tachyzoites that disseminate throughout the host infecting various organs. In immunocompetent individuals, tachyzoites differentiate into slow-growing bradyzoites, forming dormant tissue cysts in muscle and immunologically privileged sites such as the central nervous system and the eye [5].

 doi:10.20944/preprints202604.0997.v1

These cysts establish chronic infection [1,6]. Clinically severe toxoplasmosis primarily affects immunocompromised hosts due to uncontrolled tachyzoite replication or reactivation of latent infection. Primary infection during pregnancy can lead to congenital toxoplasmosis often resulting in abortion, stillbirth, or severe developmental abnormalities in the fetus [7,8]. Current treatment options are limited by toxicity, poor tolerability, and incomplete efficacy against chronic tissue cysts [9]. The absence of safe, well-tolerated, and cyst-targeting drugs underscores the critical need for the development of novel anti-*Toxoplasma* compounds with enhanced efficacy, reduced side effects, and activity against both acute and chronic stages of the parasite.

Bumped kinase inhibitors (BKIs) represent a promising class of compounds with antiprotozoal activity and in vivo safety [10–12]. BKIs were designed based on a pyrazolopyrimidine (PP) or a 5-aminopyrazole-4-carboxamide (AC) scaffold, representing two principal chemical backbones within this compound class [10,11]. Compounds have been optimized to selectively target calcium-dependent protein kinase 1 (CDPK1), a kinase conserved among apicomplexans but absent in mammalian hosts [11,13]. Exploiting the naturally occurring small gatekeeper residue in the ATP-binding of apicomplexan CDPK1 enables selective inhibition, since mammalian kinases have a bulkier gatekeeper residue preventing BKI binding [11]. Calcium signaling pathways are crucial in apicomplexan parasites, and CDPK1 is required for critical cellular processes such as microneme secretion, gliding motility, host cell invasion, egress [14,15], cytokinesis, intracellular proliferation and stage conversion [16]. Recent studies have revealed that BKIs also inhibit *T. gondii* mitogen-activated protein kinase–like 1 (TgMAPKL1), a kinase that regulates centrosome duplication and is essential for proper endodyogeny [17]. Mutations in TgMAPKL1 disrupt cell division, compromising parasite replication[18]. Moreover, it has been reported that *in vitro* treatment of several apicomplexans cultured in HFF or in monkey kidney epithelial cell line (MARC) with various BKIs not only impaired egress and host cell invasion but also induced the transformation of intracellular tachyzoites into schizont-like multinucleated complexes (MNCs) [12,19]. These MNCs are characterized by: i) continuous nuclear division without complete cytokinesis; ii) accumulation of newly formed intracellular zoites not fully individualized that lack the outer plasma membrane; iii) simultaneous display of bradyzoite and tachyzoite features, and iv) MNCs are drug induced. Unable to undergo egress from the host cell, BKI-induced MNCs persisted in vitro for extended periods and were able to reconvert to tachyzoites upon drug withdrawal. Designated “baryzoites” (from the Greek *βαρύς*, meaning massive or inert), this drug-induced stage appears to facilitate parasite survival during prolonged exposure to elevated BKI concentrations [20,21].

BKI-1708 is a bumped kinase inhibitor with a 5-aminopyrazole-4-carboxamide (AC) scaffold [10]. It has been shown to be effective and safe *in vitro* and *in vivo* in pregnant mice infected with *T. gondii* and *Neospora caninum* [22], and is also highly effective against *Cryptosporidium parvum* infection in neonatal mouse and calf models [23], although in *Cryptosporidium* no MNCs were formed. Recently, a comparative study on baryzoites induced by BKI-1708 in the closely related cyst-forming apicomplexans *T. gondii*, *N. caninum* and *B. besnoiti* reported common, but also distinguishing features in the three species [24]. TEM analysis showed that all three formed viable MNCs that remained trapped inside the host cells, but an electron-dense cyst wall-like structure was reported only in *T. gondii* baryzoites, and species-specific differences in antigen expression were observed by immunofluorescence. Comparative proteomic analysis revealed a downregulation of ribosomal proteins, proteins associated with secretory organelles, as well as of transcription and translation factors in baryzoites across all species. Bradyzoite-specific markers were upregulated only in *T. gondii* baryzoites [24]. While BKI-1708 has been shown to target CDPK1 and MAPKL1, its precise molecular mechanism of action remains to be completely resolved and potential effects on part of the host cells have not been thoroughly evaluated.

To define putative molecular targets in both parasite and host contexts, drug affinity chromatography coupled to mass spectrometry (DAC-MS) was performed. DAC-MS is a chemo-proteomic approach in which the compound of interest is immobilized on a solid matrix and used to enrich interacting proteins from complex lysates, followed by mass spectrometric identification. This

 doi:10.20944/preprints202604.0997.v1

strategy enables unbiased capture of both direct binders and associated protein complexes [25]. BKI-1708 shares a quinoline core structure scaffold with structural similarities to the first-generation antiprotozoal quinine, a compound historically linked to significant off-target effects – a side-by-side structural representation further emphasizes the potential for broader target engagement beyond canonical kinase inhibition [26,27]. An earlier DAC-MS study on cell free extracts of *N. caninum* and *Danio rerio* employing BKI-1748, a compound closely related to BKI-1708, and quinine, showed that a majority of BKI-1748 binding proteins were involved in nucleic acid binding and modification, in particular, RNA splicing and key steps of intermediate metabolism [27]. Moreover, BKI-1748 DAC-MS of extracts of *C. parvum* and in human colon tumor (HCT) host cells revealed the presence of RNA-binding and ribosomal proteins involved in translation and RNA processing in parasite and in host cell eluates from both BKI-1748 and quinine columns, but failed to identify any *C. parvum* proteins binding specifically to BKI-1748 and not to quinine [28]. These results suggested that the molecular interactions of BKI-1748 are not limited to specific targets in apicomplexans such as CDPK1 and MAPKL1, but also to host cell proteins, which are involved in common, essential pathways. This aligns with the evolving paradigm shift from the classical "one drug–one target" model toward a systems-level view, in which a compound engages a network of proteins rather than a single defined enzyme [25]. Evidence from various drug-adapted *T. gondii* strains further supports this concept, demonstrating that resistance to antiprotozoal drugs frequently involves coordinated alterations in multiple proteins and compensatory pathways rather than a single target mutation [29,30]. Here we present the identification of molecular targets of compound BKI-1708 identified by DAC-MS in both *T. gondii* ME49 tachyzoites and *T. gondii*-infected and non-infected human fibroblast host cells (HFF).

2. Materials and Methods

2.1. Parasites, Culture Medium, Biochemicals and Compounds

If not stated otherwise, all tissue culture media were purchased from Gibco-BRL (Zürich, Switzerland) and biochemicals from Sigma (St. Louis, MO, USA). BKI-1708 was synthesized in the Department of Biochemistry of the University of Washington, USA **[11]** and scaled up by WuXi Apptec Inc., Wuhan, China to >98% purity by LC/MS-MS and NMR, being provided as powder stored at room temperature. Human foreskin fibroblasts (HFF; ATCC, PCS-201-010TM) were maintained in Dulbecco's modified Eagle medium (DMEM) supplemented with 10% heat-inactivated and sterile filtered fetal calf serum (FCS), 50 U of penicillin/ml, and 50 µg streptomycin/ml. *T. gondii* ME49 tachyzoites were cultured as previously described **[19]**. The chemical structures of BKI-1708 and quinine were designed using ACD/ChemSketch (Freeware) version 2025.2.1.

2.2. SEM and TEM of T. gondii Baryzoites Formed Upon Exposure to BKI-1708.

Drug treatments and preparation for TEM and SEM were done as described by [24]. HFF were grown to confluence in T25 flasks in culture medium at 37 °C/5% CO_2 and were infected with 1 × 10^6 *T. gondii* ME49 tachyzoites. At 4 h post-infection, the medium was supplemented with 2.5 µM BKI, or not. Medium was removed after 48 h for untreated cultures, or after 6 days continuous BKI-1708 treatment. Subsequently, cultures were fixed for TEM and SEM, and processed and embedded in Epon 812 epoxy resin (Sigma (St. Louis, MO, USA)[24]. Sections of 80 nm thickness were cut on an ultramicrotome (Reichert and Jung, Vienna, Austria) and were transferred onto formvar–carbon-coated 200 mesh nickel grids (Plano GmbH, Marburg, Germany). They were stained with Uranyless® and lead citrate (Electron Microscopy Sciences, Hatfield PA, USA), and specimens were inspected on a FEI Morgagni TEM equipped with a Morada digital camera system (12 Megapixel) operating at 80 kV.

 doi:10.20944/preprints202604.0997.v1

2.3. Protein Extraction and Differential Affinity Chromatography (DAC)

For protein extraction, frozen pellets of *T. gondii* ME49 tachyzoites were resuspended in ice-cold extraction buffer, i.e., PBS (phosphate buffered saline) containing 1% Triton X-100 and 1% of Halt proteinase inhibitor cocktail (ThermoFisher). Suspensions were vortexed thoroughly and centrifuged (13,000 rpm, 10 min, 4 ◦C). Extraction of pellets was repeated twice. Four ml of extraction buffer was used in total. Supernatants were combined (resulting in approximately 3 mg of total protein) and subjected to affinity chromatography. To produce the sepharose matrices conjugated to BKI-1708 or quinine 0.5 g of lyophilized epoxy-sepharose with a C12 spacer was suspended in 15 mL H2O and centrifuged at 300× g for 5 min. Washes in water were repeated twice followed by a wash with coupling buffer (0.1 M NaHCO3, pH 9.5). After the last wash, 20 mg of each compound dissolved in 2.5 mL DMSO (dimethylsulfoxide) were added, and coupling buffer was added to a maximum volume of 5 mL. Mock column medium was generated by incubating 0.5 g of epoxy-sepharose with DMSO. The mixture was incubated for 3 days at 37 ◦C under slow but continuous shaking to allow coupling of the epoxy group to the compounds. The resulting column medium (approximately 2 mL) was washed with coupling buffer (15 mL) followed by a wash with ethanolamine (1 M, pH 9.5) and by an incubation in 10 mL of ethanolamine for 4 h at 20 ◦C in the dark to block residual reactive groups. Then, the column medium was transferred to a chromatography column (Novagen, Merck, Darmstadt, Germany) and extensively washed with PBS-DMSO (1:1) and PBS to remove unbound compounds. The columns were stored in PBS containing 0.02% NaN3 at 4 ◦C. Prior to affinity chromatography, mock columns were combined to columns in tandem (mock first, then compound) and washed with 50 mL PBS equilibrated at 20 ◦C.

For DAC, mock and compound columns were mounted in parallel. In order to simultaneously obtain quinine and BKI-1708 binding proteins, 2 ml aliquots of crude extracts were loaded in parallel on the mock columns on top of the quinine and BKI-1708 columns and allowed to percolate through the tandem by gravity flow. Subsequently, the tandem was washed with 25 ml PBS equilibrated at 20 °C. Then, the columns were separated, and bound proteins were eluted with 50 mM acetic acid (5 mL per column) by gravity flow. The eluates were lyophilized, and the lyophilizates were stored at −80 ◦C.

2.4. Proteomic Analysis of the Eluted Proteins by Mass Spectrometry

The lyophilized residues were resuspended in 10 µL of 8M urea and 0.1 M of Tris-HCl^- (pH = 8), and sonication in a water bath for 5 min. Proteins were reduced and alkylated with 10 mM dithiothreitol for 30 min at 37 °C and 50 mM of iodoacetamide for 30 min at room temperature. Iodoacetamide was quenched by the addition of 5 µL 0.1 M dithiothreitol in 0.1 M of Tris-HCl^- (pH = 8) and the urea concentration was diluted to 4 M by the addition of 2 mM Calcium dichloride in 20 mM Tris buffer. Proteins were double-digested for 2 hours at 37° with 1 µL of 0.1 µg/µL LysC sequencing grade protease (Promega), followed by further dilution of urea to 1.6 M and 1 µL of 0.1 µg/µL trypsin sequencing grade (Promega) over night at room temperature. Digestion was stopped with 1% (v/v) trifluoroacetic acid end concentration. The digest was spun for 1 min at 16,000 g, after an incubation for 15 min at room temperature, and the cleared supernatant was transferred to a HPLC vial for subsequent nano-liquid reversed phase chromatography coupled to tandem mass spectrometry on a system consisting of a nanoElute 2 ultra-performance liquid chromatograph coupled to a trapped ion mobility spectrometry-time of flight mass spectrometer (timsTOF HT; Bruker Daltonics, Bremen, Germany), through a CaptiveSpray source (Bruker Daltonics, Bremen, Germany) with an end-plate offset of 500 V, a drying temperature of 200 °C, and with the capillary voltage fixed at 1.6 kV. A volume of 2µL protein digest were loaded onto a pre-column (C18 PepMap 100, 5µm, 100A, 300µm i.d. x 5mm length, ThermoFisher Scientific, Waltham, USA) at a pressure of 80bars with 0.05% TFA in water/acetonitrile 98:2. After loading, peptides were eluted in back flush mode onto a PepSep column (150 µm × 15 cm, PepSep, Odense, Denmark) applying a 30 min active peptide separation gradient at a flow rate 500 nL/min. Data were acquired in data-dependent acquisition (DDA) method employing eight parallel accumulation-serial fragmentation ramps in the

 doi:10.20944/preprints202604.0997.v1

ion mobility range of 0.75 to 1.35 1/k0, m/z range between 100–1700 u at a cycle time of 0.95 sec at 300Hz acquisition rate.

The mass spectrometry data were searched and quantified with FragPipe, version 22.0 [31] against *T. gondii* ME49 annotated protein sequences concatenated with the Swissprot human sequences release from 2025_01 and some common contaminants, including trypsin/LysC, keratins, bovine serum albumin, etc., and their corresponding reversed sequences. Search parameters included Acetyl (Protein N-term) and Oxidation (M) as variable modifications (3 max variable modifications), Carbamidomethyl (C) as fixed modification, and Trypsin/P (max 3 missed cleavages) as digestion enzyme. MSBooster called the Prosit_2019_irt and Prosit_2023_intensity_timsTOF retention time and spectra prediction models, then peptide spectrum matches, peptides and proteins were filtered to a 1% false discovery rate using percolator and protein prophet. Protein groups with less than two peptides per group were excluded from further data consideration. The leading protein selected by protein prophet was chosen per protein group to calculate an IBAQ (intensity-based absolute quantification) value [32]. From IBAQ values relative abundance (rAbu) was calculated so that the sum of all rAbu were 1000000 for each sample. The putative functions of identified proteins were identified based on information given by Uniprot (www.uniprot.org), Toxo DB (https://toxodb.org) and related databases.

3. Results

3.1. Exposure of T. gondii Tachyzoites to BKI-1708 Initiates Baryzoite Formation

HFF were infected with *T. gondii* tachyzoites, and at 4 h post-infection cultures were treated with 2.5 μM BKI-1708 for a period of 6 days. Control cultures were maintained for 48 h in the absence of compound. The resulting baryzoites that were formed upon exposure to BKI-1708 are shown in Figure 1 A–D. They form a bulky mass containing numerous nuclei, indicating the DNA replication and nuclear division is maintained. They had different shapes and sizes, often with protruding apical complexes of newly formed zoites pointing outwards. Baryzoites were always surrounded by a triple membrane as found in non-treated tachyzoites, but the internal zoites were clustered together, being inhibited in the completion of cytokinesis at a final stage. They were unable to dissociate from each other and thus remained intracellular. The parasitophorous vacuole containing *T. gondii* baryzoites formed a peripheral electron dense layer reminiscent of tissue cyst wall formation, most likely built up by secretory components secreted into the matrix of the parasitophorous vacuole. In the absence of compound (Figure 1 E and F), tachyzoites proliferated rapidly, forming large parasitophorous vacuoles containing numerous individual daughter tachyzoites ready to undergo egress and to infect neighboring host cells.

3.2. DAC-Overview

Differential affinity chromatography (DAC) was performed using BKI-1708 as the compound of interest and quinine as differential compound given its similarity to BKI-1708 due to a common quinoline core. The two compound structures are shown in Figure 2.

Mass spectrometry analysis of the proteomes obtained after DAC of cell free-extracts from *T. gondii* ME49 tachyzoites and HFF yielded overall 14897 unique peptides matching 453 *T. gondii* proteins and 9873 unique peptides matching 831 host cell proteins. The complete datasets for HFF (infected and non-infected) and *T. gondii* are provided in Tables S1 and S2, respectively. Visualization of the protein intensity distributions (PID) by box plots show that they exhibit some degree of variation between the different samples (see Supplementary Figure 1), and hierarchical clustering shows that that infected segregated significantly from non-infected samples (Supplementary Figure 2).

 doi:10.20944/preprints202604.0997.v1

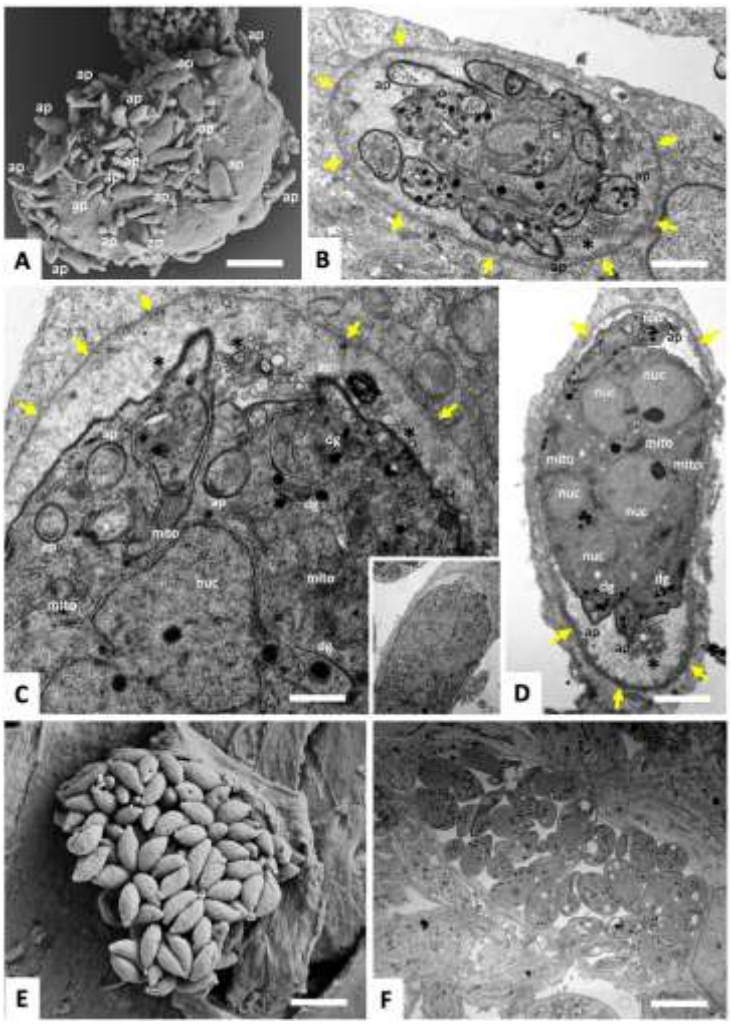

Figure 1. Baryzoite formation in *Toxoplasma gondii* induced by BKI-1708. (**A-D)** show infected HFF that were treated with 2.5 µM BKI-1708 starting at 4 h post-infection, and were maintained for 6 days prior to processing for SEM **(A)** and TEM **(B-D), (C)** contains an insert that provides a lower magnification view of the MNC. (**E**, **F)** show non-treated controls with tachyzoites situated within a parasitophorous vacuole, fixed and processed for SEM and TEM, respectively, after 48 h of culture; nuc = nucleus, ap = apical parts of newly formed zoites; dg = dense granule; rop = rhoptries; arrows point towards electron dense cyst wall-like structure forming in the parasitophorous vacuole periphery; * indicates secreted material in the vacuole matrix. Bars in A = 5 µm, B = 1.9 µm, C = 0.9 µm, D = 2.6 µm, E = 5 µm, F = 4.2 µm.

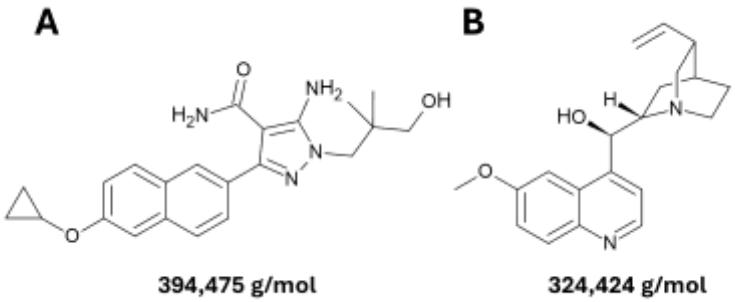

Figure 2. Chemical structures of BKI-1708 (A) and quinine (B) and their respective molecular weights. JM: better in Materials and Methods.

 doi:10.20944/preprints202604.0997.v1

3.3. T. gondii Proteins Binding Identified by BKI-1708 DAC-MS

A total of 453 *T. gondii* ME49 proteins were identified by DAC (Figure 3; Table S1). The largest subset of 205 proteins was commonly identified in eluates from BKI-1708, quinine and mock columns. Out of the proteins that were not captured by the mock column, 35 proteins were specifically eluted from the BKI-1708 column, and they are shown in (Table 1). A total of 132 proteins were detected in the quinine-binding fraction, of which 58 were also identified in the BKI-1708 column fraction (Table 2), and 74 proteins were found to bind specifically to quinine.

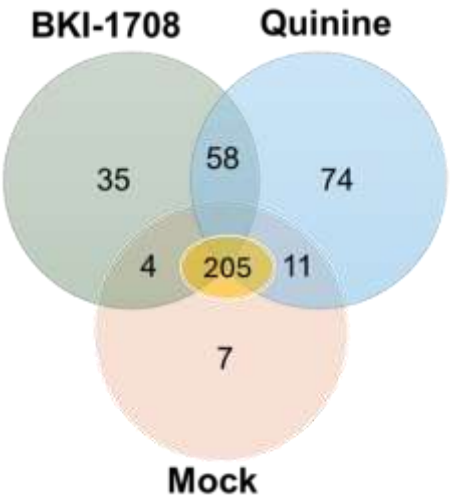

Figure 3. Venn diagram detailing the number of proteins identified by DAC in cell-free extracts of *T. gondii* ME49 tachyzoites. Eluates from BKI-1708 and quinine columns were compared by MS shotgun analysis as described in Materials and Methods. The numbers of the proteins within the subsets are explained in detail in the text.

The proteins binding specifically to BKI-1708 were implicated in a variety of cellular functions and pathways linked to cell division, cytoskeleton, vesicular trafficking, secretory organelles, detoxification and transcriptional and translational regulators (Table 1). Among those, mitochondrial peroxiredoxin 3 (TgPrx3), which is involved in managing oxidative stress and modulates the immune response during infection [33], exhibited the by far highest relative abundance, followed by the putative protein transport TgSEC31.

Table 1. List of the 35 *T. gondii* ME49 proteins specifically binding to BKI-1708. The relative abundances (rAbu) based on iBAQ sum up to a total of 1,000,000 for each sample. The proteins are listed according to their decreasing rAbu values.

Toxo DB ORF	Annotation	rAbu
TGME49_230410	peroxiredoxin PRX3	604.9
TGME49_311400	protein transport protein SEC31, putative	368.6
TGME49_290920	oxidoreductase, 2OG-Fe(II) oxygenase family protein	251.6
TGME49_209420	hypothetical protein	248.3
TGME49_201700	protein transport protein SEC13	232.4
TGME49_224720	SPOC domain-containing protein	216.6
TGME49_205180	RNA recognition motif-containing protein	190.9
TGME49_313270	hypothetical protein	174.3
TGME49_320600	cold-shock DNA-binding domain-containing protein	172.5
TGME49_232370	CW-type Zinc Finger protein	160.7

 doi:10.20944/preprints202604.0997.v1

TGME49_273960	chaperonin GroS protein	151.5
TGME49_231440	LsmAD domain-containing protein	137.2
TGME49_294670	eukaryotic translation initiation factor 3 subunit G, putative	127.0
TGME49_263530	chaperonin, putative	91.1
TGME49_265250	RNA recognition motif-containing protein	84.3
TGME49_202780	rhoptry kinase family protein ROP25	74.6
TGME49_250830	26S proteasome regulatory subunit RPN12, putative	73.9
TGME49_201760	thioredoxin-like associated protein TLAP4	61.1
TGME49_218240	inner membrane complex protein IMC25	54.4
TGME49_278975	metacaspase MCA2	51.5
TGME49_205320	hypothetical protein	48.2
TGME49_291680	protein transport protein SEC23, putative	44.4
TGME49_309200	zinc finger (CCCH type) motif-containing protein	41.6
TGME49_204160	GYF domain-containing protein	39.1
TGME49_269690	dense granule protein GRA29	36.0
TGME49_250115	hypothetical protein	21.1
TGME49_204130	perforin-like protein PLP1	20.0
TGME49_232280	hypothetical protein	18.6
TGME49_215360	dense granule protein GRA62	17.9
TGME49_258240	chromodomain helicase DNA binding protein CHD1/SWI2/SNF2	10.7
TGME49_298610	GYF domain-containing protein	9.6
TGME49_233120	AP2 domain transcription factor AP2VIII-2	8.6
TGME49_253750	PLU-1 family protein	7.3
TGME49_254940	MIF4G domain-containing protein	7.3
TGME49_244500	Tubulin-tyrosine ligase family protein	2.8

The 58 proteins retained by both BKI-1708 and quinine (20 of which are listed in Table 2) are involved in RNA metabolism including splicing, translation, and ribosome biogenesis. This includes multiple RNA-binding proteins (RRM- and LSM domain–containing proteins), pre-mRNA processing factors (splicing factor 3b, TgPRPF19), nucleosome assembly protein (TgNAP), ribosome biogenesis regulators (TgRRS1, TgNOL1/NOP2), ribosomal protein TgL1, and rRNA pseudouridine synthase; and several components of the translation initiation machinery (TgeIF3 subunits E, 3, 7, 10; IF-2; TgeIF3 subunit 6–interacting protein), elongation-related factors (TgEF-1 GEF domain protein) and tRNA-associated proteins (tRNA import protein, glutamate-tRNA ligase). In addition, this fraction also contains proteins linked to energy metabolism and mitochondria (ATP synthase subunits α, β, F1γ; TgSDHB), cytoskeletal/structural elements (Tgcentrin 3, TgIMC33), vesicular trafficking (clathrin light chain and adaptor complex proteins), signaling/regulation (Tg14-3-3, TgCK2 kinase, TgRCC1, TgPPM3C), and secretory organelles (TgGRA23, TgGRA30, TgAMA1). The protein with the highest abundance is a hypothetical protein (TGME49_201860), whose expression levels were downregulated in *T. gondii* baryzoites [24].

Table 2. List of the 20 most abundant *T. gondii* ME49 proteins binding to both BKI-1708 and quinine columns. The relative abundances (rAbu) based on iBAQ sum up to a total of 1,000,000 for each sample. The proteins are listed according to their decreasing rAbu values in BKI-1708 eluates.

Toxo DB ORF	Annotation	rAbu BKI-1708	rAbu Quinine

 doi:10.20944/preprints202604.0997.v1

TGME49_201860	hypothetical protein	1185.1	600.9
TGME49_205558	NAC domain-containing protein	827.0	53.9
TGME49_244110	nucleosome assembly protein (nap) protein	300.3	34.8
TGME49_314830	pre-mRNA splicing factor subunit, putative	202.3	160.9
TGME49_232000	dense granule protein GRA30	190.2	43.6
TGME49_248250	translation initiation factor IF-2, putative	175.8	376.6
TGME49_294970	hypothetical protein	156.6	38.8
TGME49_265530	RNA recognition motif-containing protein	130.9	8.9
TGME49_257380	inhibitor of cysteine protease 1	122.5	181.9
TGME49_263090	14-3-3 protein	115.4	50.4
TGME49_500284	hypothetical protein, conserved	88.8	13.9
TGME49_291330	RNA recognition motif-containing protein	88.1	105.8
TGME49_260670	centrin 3	86.9	61.6
TGME49_213030	clathrin light chain, putative	84.2	437.1
TGME49_213940	CHCH domain-containing protein	78.1	35.8
TGME49_280550	clathrin adaptor complex small chain subfamily protein	74.7	77.3
TGME49_300280	LSM domain-containing protein	64.5	48.0
TGME49_269180	MIF4G domain-containing protein	60.4	4.5
TGME49_213050	hypothetical protein	60.2	41.2
TGME49_313640	hypothetical protein	51.6	166.6

3.4. DAC-MS Revealed Distinct BKI-1708 affino-Proteomes in T. gondii-Infected and Non-Infected HFF

Amongst a total of 831 human host cell proteins identified by DAC, 397 proteins were not found in mock column eluates. Subsets of specific compound-binding proteins identified in infected and non-infected cells are shown in Figure 4. BKI-1708 interacted with distinct protein subsets depending on the infection status of HFF: in non-infected cells, 20 proteins were specifically engaged, whereas 8 proteins were exclusive to infected HFF. A set of 12 proteins was shared between both conditions, representing a core of infection-independent binders. Overlap with quinine controls was minimal, with only 9 proteins common to all conditions.

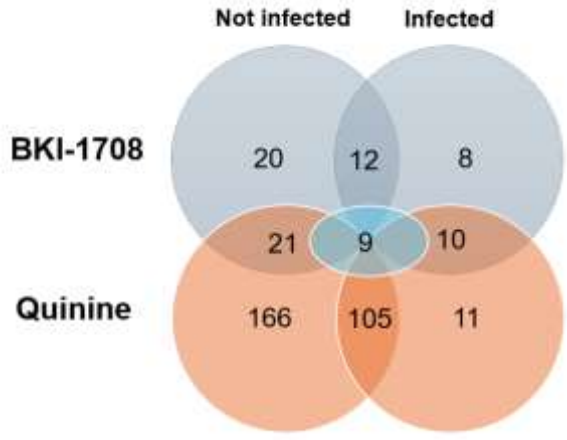

 doi:10.20944/preprints202604.0997.v1

Figure 4. Venn diagram detailing the number of HFF proteins identified by DAC in cell-free extracts of not infected and infected cells. Eluates from BKI-1708 and quinine columns were compared by MS shotgun analysis as described in Materials and Methods. The numbers of the proteins within the subsets are explained in detail in the text.

3.4.1. Host Cell Proteins Identified by BKI-1708 DAC-MS in Non-Infected HFF

First, DAC-MS was performed using extracts from non-infected HFF. The largest subset of proteins, namely 166, was identified exclusively in eluates from quinine columns. The full list of proteins can be accessed in Table S1. Overall, quinine-specific binding proteins included 21 ribosomal proteins, 3 Rab proteins, and 25 transport-related proteins involved in protein synthesis and trafficking. Additionally, 34 proteins identified were associated with the cytoskeleton, including actin, tubulin, catenins, and myosins, while 43 proteins are involved in phosphorylation, dephosphorylation, signal relay, GTP-binding, and receptor activity. Fifteen proteins of the total subset were linked to energy metabolism. Fractions containing proteins binding to both, BKI-1708 and to quinine, contained a clearly diminished subset of 21 binding proteins (Table 3), and the fraction of proteins binding specifically to BKI-1708 was comprised of 20 proteins (Table 4).

Table 3. List of host cell proteins binding to BKI-1708 and quinine in non-infected cells. The relative abundances (rAbu) based on iBAQ sum up to a total of 1,000,000 for each sample. The proteins are listed according to their decreasing rAbu values in BKI-1708 column eluates of non-infected cells.

Protein ID	Annotation	rAbu BKI-1708	rAbu Quinine
P47756	F-actin-capping protein subunit beta	164.5	663.0
P55735	Protein SEC13 homolog	161.5	351.3
Q9NR12	PDZ and LIM domain protein 7	156.5	210.0
P52907	F-actin-capping protein subunit alpha-1	147.5	741.8
Q07021	Complement component 1 Q subcomponent-binding protein, mitochondrial	135.2	151.0
Q8WX93-3	Isoform 3 of Palladin	109.7	11.8
P51608-2	Isoform B of Methyl-CpG-binding protein 2	92.1	45.6
P09493-8	Isoform 8 of Tropomyosin alpha-1 chain	71.6	463.0
P51659	Peroxisomal multifunctional enzyme type 2	60.5	18.0
Q96GY0	Zinc finger C2HC domain-containing protein 1A	60.3	31.4
Q9C0C2	182 kDa tankyrase-1-binding protein	50.5	160.2
Q8ND56-2	Isoform 2 of Protein LSM14 homolog A	49.4	64.1
Q16531	DNA damage-binding protein 1	35.4	18.0
Q13428-2	Isoform 2 of Treacle protein	31.0	143.0
Q9HAU0-2	Isoform 2 of Pleckstrin homology domain-containing family A member 5	28.7	63.5
Q14974	Importin subunit beta-1	18.6	449.9
P08123	Collagen alpha-2(I) chain	15.2	20.9
P50281	Matrix metalloproteinase-14	12.1	55.5
P49821-2	Isoform 2 of NADH dehydrogenase [ubiquinone] flavoprotein 1, mitochondrial	11.6	25.4
O60664-3	Isoform 3 of Perilipin-3	9.3	192.6

 doi:10.20944/preprints202604.0997.v1

O14974-5	Isoform 5 of Protein phosphatase 1 regulatory subunit 12A	9.2	185.0

Table 4. List of host cell proteins specifically binding to BKI-1708 columns in non-infected cells. The relative abundances (rAbu) based on iBAQ sum up to a total of 1,000,000 for each sample. The proteins are listed according to their decreasing rAbu values.

Protein ID	Annotation	rAbu
Q9Y2S6	Translation machinery-associated protein 7	5041.5
P16949-2	Isoform 2 of Stathmin	1608.4
P55000	Secreted Ly-6/uPAR-related protein 1	324.7
P50995-2	Isoform 2 of Annexin A11	286.3
P82909	Alpha-ketoglutarate dehydrogenase component 4	195.2
Q96FJ2	Dynein light chain 2, cytoplasmic	160.2
P01036	Cystatin-S	157.5
P62633-2	Isoform 2 of CCHC-type zinc finger nucleic acid binding protein	128.7
Q01105	Protein SET	77.4
O00151	PDZ and LIM domain protein 1	66.2
P61964	WD repeat-containing protein 5	62.6
P11137-2	Isoform 2 of Microtubule-associated protein 2	61.7
Q6UUV7-3	Isoform 3 of CREB-regulated transcription coactivator 3	57.6
Q16555-2	Isoform 2 of Dihydropyrimidinase-related protein 2	49.7
Q9P270	SLAIN motif-containing protein 2	47.5
O94979-10	Isoform 10 of Protein transport protein Sec31A	40.5
P20073-2	Isoform 2 of Annexin A7	30.0
P78344	Eukaryotic translation initiation factor 4 gamma 2	27.7
P04040	Catalase	26.7
P27816-5	Isoform 5 of Microtubule-associated protein 4	24.6

The three most abundant HFF proteins binding to both BKI-1708 and quinine (Table 3) were F-actin-capping protein subunit beta (CAPZB) and PDZ and LIM domain protein 7 (PDLIM7), and the nuclear transport protein protein SEC13 homolog (SEC13) .

Out of the total of twenty proteins found interacting exclusively with BKI-1708 in non-infected cells (Table 4), the most abundant protein found was translation machinery-associated protein 7 (TMA7); followed by Stathmin (STMN1). In addition, several BKI-1708 specific binding proteins are involved in cytoskeletal regulation and intracellular trafficking, including i) PDZ and LIM domain protein 1 (PDLIM1), ii) isoform 2 of Dihydropyrimidinase-related protein 2 (DPYSL2); iii) isoform 10 of protein transport protein Sec31A (Sec31A); iv) SLAIN motif-containing protein 2 (SLAIN2), and v) microtubule-associated proteins 4 (MAP4) and 2 (MAP2). Furthermore, annexins A11 and A7 (ANXA11, ANXA7) were also identified as BKI-1708 specific binders. Identified BKI-1708 binders directly involved in RNA-related processes include RNA-binding CCHC-type zinc finger nucleic acid binding protein (CNBP), and eukaryotic translation initiation factor 4 gamma 2 (eIF4G2). Furthermore, two proteins with DNA-binding functions were identified in BKI-1708 affino-proteome dataset: WD repeat-containing protein 5 (WDR5) and Protein SET (SET). The third most abundant identified protein is Secreted Ly-6/uPAR-related protein 1 (SLURP1). in addition, CREB-regulated transcription coactivator 3 (CRTC3), was identified as protein binding specifically to BKI-1708. Lastly, Catalase (CAT), which regulates the degradation of hydrogen peroxide, was found to bind specifically to BKI-1708 (Table 4).

3.4.2. Proteins Identified by BKI-1708 DAC-MS in T. gondii Infected HFF

 doi:10.20944/preprints202604.0997.v1

In *T. gondii* infected host cells, the number of proteins binding to BKI-1708 was markedly reduced when compared to non-infected conditions. Specifically, eight proteins were found to interact exclusively with BKI-1708, eleven bound only to quinine, and ten were identified in both BKI-1708 and quinine column eluates (Figure 4, Tables 5, 6).

Amongst the 8 host proteins uniquely associated with BKI-1708 in infected cells, the most abundant was the secreted protein-binding extracellular glycoprotein lacritin (LACRT) (Table 5), followed by isoform 2 of polyglutamine-binding protein 1 (PQBP1-2). Beyond these, the proteins binding exclusively to BKI-1708 in infected cells were associated with nucleic acid and protein metabolism, with only a single protein (mitochondrial L-lactate dehydrogenase B chain (LDHB) linked to energy metabolism. Moreover, two nuclear proteins were detected: isoform 2 of nuclear pore complex protein Nup153 (NUP153) and isoform 2 of pescadillo homolog (PES1). Other pulled-down proteins with RNA-binding activities include i) Isoform 2 of Myb-binding protein 1A (MYBBP1A) and ii) Isoform 2 of proliferation marker protein Ki-67 (MKI67). Lastly, isoform 2 of suprabasin (SBSN) was identified.

Table 5. List of proteins specifically binding to BKI-1708 in *T. gondii* infected HFF. The relative abundances (rAbu) based on iBAQ sum up to a total of 1,000,000 for each sample. The proteins are listed according to their decreasing rAbu values in BKI-1708 eluates of infected cells.

Protein ID	Annotation	rAbu
Q9GZZ8	Extracellular glycoprotein lacritin	244.7
O60828-2	Isoform 2 of Polyglutamine-binding protein 1	76.5
P07195	L-lactate dehydrogenase B chain	43.1
Q6UWP8-2	Isoform 2 of Suprabasin	26.1
P49790-2	Isoform 2 of Nuclear pore complex protein Nup153	23.7
O00541-2	Isoform 2 of Pescadillo homolog	23.6
Q9BQG0-2	Isoform 2 of Myb-binding protein 1A	22.6
P46013-2	Isoform Short of Proliferation marker protein Ki-67	8.7

Table 6. List of proteins of *T. gondii*-infected HFF binding to both BKI-1708 and quinine. The relative abundances (rAbu) based on iBAQ sum up to a total of 1,000,000 for each sample. The proteins are listed according to their decreasing rAbu values in BKI-1708 eluates of infected cells.

Protein ID	Annotation	BKI-1708 rAbu	Quinine rAbu
P11387	DNA topoisomerase 1	97.2	27.2
Q9NX24	H/ACA ribonucleoprotein complex subunit 2	85.5	98.7
O75400-2	Isoform 2 of Pre-mRNA-processing factor 40 homolog A	45.0	7.0
Q9NXV6	CDKN2A-interacting protein	30.4	9.7
P78316	Nucleolar protein 14	21.4	5.7
P31943	Heterogeneous nuclear ribonucleoprotein H	17.1	139.2
Q8NDZ4	Divergent protein kinase domain 2A	16.7	2.8
P00750-2	Isoform 2 of Tissue-type plasminogen activator	12.3	17.4
O94776-2	Isoform 2 of Metastasis-associated protein MTA2	11.1	15.3
Q8WUM4-2	Isoform 2 of Programmed cell death 6-interacting protein	10.3	2.4

3.4.3. Host Cell Proteins Binding Exclusively to BKI-1708 in Both T. gondii-Infected and Non-Infected HFF

 doi:10.20944/preprints202604.0997.v1

Twelve proteins were found to bind specifically to BKI-1708 in both infected and non-infected cells – mostly RNA-binding proteins (Table 7). Zinc finger protein 706 and Isoform 2 of splicing factor 1 (SF1) were the most abundant BKI-binder protein detected in both eluates.

Table 7. List of proteins binding exclusively to BKI-1708 in both *T. gondii*-infected and non-infected HFF. The relative abundances (rAbu) based on iBAQ sum up to a total of 1,000,000 for each sample. The proteins are listed according to their decreasing rAbu values in BKI-1708 eluates of non-infected cells.

Protein ID	Annotation	rAbu non-infected	rAbu infected
Q9Y5V0	Zinc finger protein 706	645.0	55.9
Q15637-2	Isoform 2 of Splicing factor 1	456.8	584.5
P78406	mRNA export factor RAE1	257.1	136.8
Q6E0U4-16	Isoform 16 of Dermokine	228.9	127.8
O43684-2	Isoform 2 of Mitotic checkpoint protein BUB3	213.9	44.1
Q13492-2	Isoform 2 of Phosphatidylinositol-binding clathrin assembly protein	194.8	66.7
O75223-3	Isoform 3 of Gamma-glutamylcyclotransferase	192.0	149.3
Q9NPA8-2	Isoform 2 of Transcription and mRNA export factor ENY2	171.9	101.7
Q8WWM7-2	Isoform 2 of Ataxin-2-like protein	157.0	167.9
P0CG12	Decreased expression in renal and prostate cancer protein	75.6	30.3
P22234-2	Isoform 2 of Bifunctional phosphoribosylaminoimidazole carboxylase/phosphoribosylaminoimidazole succinocarboxamide synthetase	15.3	51.0
Q96AE4-2	Isoform 2 of Far upstream element-binding protein 1	13.7	154.3

3.4.4. Host Cell Proteins Binding to Both BKI-1708 and Quinine in T. gondii-Infected and Non-Infected HFF

In addition, a subset of nine proteins was identified in all column eluates, interacting with BKI-1708 and quinine in both infected and non-infected cells (Table 8), including RNA-binding and proteins associated with cytoskeletal organization and intracellular transport and with functions in redox homeostasis.

Table 8. List of proteins binding to BKI-1708 and quinine in both non-infected and *T. gondii*-infected HFF. The relative abundances (rAbu) based on iBAQ sum up to a total of 1,000,000 for each sample. The proteins are listed according to their decreasing rAbu values in BKI-1708 eluates of infected cells.

		Non-infected HFF	Infected HFF

 doi:10.20944/preprints202604.0997.v1

Protein ID	Annotation	BKI-1708 rAbu	Quinine rAbu	BKI-1708 rAbu	Quinine rAbu
P35637-2	Isoform Short of RNA-binding protein FUS	571.8	257.7	391.0	69.1
Q14011	Cold-inducible RNA-binding protein	506.4	299.3	203.4	63.9
Q9H0D6-2	Isoform 2 of 5′-3′ exoribonuclease 2	16.8	41.5	65.1	18.2
P63167	Dynein light chain 1, cytoplasmic	791.7	1136.8	41.2	42.5
Q9UHB6-4	Isoform 4 of LIM domain and actin-binding protein 1	8.7	584.4	20.7	2.4
Q06830	Peroxiredoxin-1	458.2	246.8	19.5	53.7
Q9UN86-2	Isoform B of Ras GTPase-activating protein-binding protein 2	41.5	81.4	15.9	16.1
P12956-2	Isoform 2 of X-ray repair cross-complementing protein 6	19.3	61.7	11.3	56.0
Q8WWI1-3	Isoform 3 of LIM domain only protein 7	20.3	137.5	6.2	1.7

3.5. Numbers and Putative Functions of T. gondii Tachzoite and HFF Proteins Specifically Binding to BKI-1708

The putative functions of proteins that specifically bind to BKI-1708 in *T. gondii* ME49 tachyzoites, as well as in infected and non-infected host cells, as well as their respective numbers, are shown in Table 9. Their functions were identified based on information available in ToxoDB (www.toxodb.org) and Uniprot (www.uniprot.org) databases.

Table 9. Summary of putative functions and respective numbers of host cell and ME49 proteins binding specifically to BKI-1708 in infected and non-infected host cells. The molecular processes assigned to the different functions are listed in Table S3.

Function	Uninfected HFF proteins	Infected HFF proteins	Infected and uninfected host cell proteins	*T. gondii* ME49 proteins
DNA binding and modification	2	3	0	5
RNA binding and modification	4	2	5	6
Protein binding and modification	3	1	1	5
Cytoskeleton and intracellular transport	6	0	1	4
Intracellular signalling	2	0	0	5
Energy and intermediary metabolism	0	1	2	2
Hypothetical or ambiguous	3	1	3	6
Total	20	8	12	35

 doi:10.20944/preprints202604.0997.v1

In *T. gondii,* the five most abundant proteins found in BKI-1708 eluates include two proteins with catalytic activity related to oxidation-reduction reactions (Peroxiredoxin PRX3 and Oxidoreductase, 2OG-Fe(II) oxygenase family protein), one hypothetical protein (TGME49_209420) and two proteins involved in protein transport (protein transport SEC31 and SEC13). Secreted proteins involved in host cell interaction and parasitism were also engaged by BKI-1708: two dense granule proteins (GRA29 and GRA62), rhoptry kinase family protein ROP25 and Perforin-like protein PLP1. Overall, *T. gondii* ME49 proteins identified interacting only with BKI-1708 cover functions related to cytoskeleton dynamics, nucleic acid binding, oxidative stress response and intracellular transport.

4. Discussion

Exposure of *T. gondii* tachyzoites to BKI-1708 induces the formation of multinucleated complexes also known as baryzoites, which represent a drug induced stage that contains newly formed zoites blocked in the final stages of cytokinesis, remaining viable for extended periods of time ([24]:). In *T. gondii,* these baryzoites form an electron-dense cyst-wall like structure situated at the periphery of the parasitophorous vacuole, which has been shown to be labelled by DBA, a known *T. gondii* cyst wall marker ([24]. In order to identify putative molecular targets of BKI-1708, BKI-1708-DAC-MS was performed on cell free extracts of *T. gondii* tachyzoites and either *T. gondii*-infected or non-infected HFF.

In *T. gondii,* the largest subset of pulled-down proteins comprises 205 proteins that bind to BKI-1708, quinine as well as the mock column, thus corresponding to non-specific binders (Figure 4). Of particular interest, 35 proteins were found exclusively in the BKI-1708 column eluates and 58 proteins were bound to both BKI-1708 and quinine columns. The 58 proteins retained by both BKI-1708 and quinine were largely involved in RNA metabolism, translation, and ribosome biogenesis. Overall, this suggests that both, BKI-1708 and quinine associate with a broad set of housekeeping processes, particularly post-transcriptional regulation and translational control, with additional links to metabolism and intracellular trafficking, and that these interactions are likely to be based on the 5-amido-caboxamide group common to both drugs. The lack of noticeable anti-parasitic activity of quinine against *T. gondii* [35] could indicate that recognition of this core motif alone is insufficient for parasite inhibition, and that additional structural features might be required.

Proteins exclusively identified in the BKI-1708 affino-proteome likely reflect additional, side-chain-mediated interactions that confer potency and/or parasite selectivity. While both BKI-1708 and quinine shared interactions with the RNA-processing and translational machinery, BKI-1708 exhibited a more pronounced association with secretory organelles, vesicular trafficking, redox regulation and parasite-specific transcriptional regulators, consistent with a more specialized and potentially invasion-related binding profile. However, the most abundant protein binding exclusively to BKI-1708 was TgPRX3 (TGME49_230410), known to have antioxidant activity [33] and involved in modulating immunopathology during *T. gondii* infection [36]. Apicomplexan parasites are subject to oxidative stress from their host cells, thus redox systems play an important role in host-pathogen interactions [37]. Other components of the BKI-1708-specific fraction are proteins with transport functions and nucleic acid-binding activities. In addition, factors known to play important roles in host cell invasion and host cell interactions and modulation, such as dense granules proteins GRA29, GRA62, rhoptry kinase family protein ROP25 and the perforin-like protein TgPLP1, were also found to bind specifically to BKI-1708. ROP and GRA proteins are known to facilitate host cell entry and modify host cell functions, and are thus important for the replication of *T. gondii* [39], while TgPLP1 is necessary for efficient parasite egress [38]. The metacaspase TgMCA2, a member of the caspase-like cysteine protease family present in plants, fungi, and protozoa, and implicated in apoptosis-like cell death in parasites, was also bound specifically to BKI-1708 [39]. Previous studies have shown that TgMCA2, in conjunction with TgMCA1, is critical for parasite replication and pathogenicity - although loss of TgMCA2 alone does not affect parasite growth, the combined deletion with TgMCA1 results in defective IMC1 maturation, impaired endodyogeny, increased bradyzoite differentiation, and reduced virulence in mice [40].

 doi:10.20944/preprints202604.0997.v1

The AP2 domain transcription factor AP2VIII-2 was also identified as a specific BKI-1708 binder. AP2 factors are central regulators of transcription in *T. gondii* and govern mechanisms that repress bradyzoite differentiation during the tachyzoite stage [41]. Although the precise role of AP2VIII-2 remains incompletely understood, recent work has shown that it partners with the ATP-dependent chromatin remodeler TgSNF2h and the scaffold protein TgRFTS to form an essential chromatin-remodeling complex that maintains transcriptional fidelity by insulating highly active genes from their silent neighbors and enabling stage-specific gene expression [42]. It is thus conceivable that disruption of AP2VIII-2 interactions could impair the complex assembly, leading to collapsing chromatin patterns, and resulting in an unstable gene expression that may slow parasite growth or induce inappropriate differentiation and developmental defects.

Furthermore, five proteins identified as specific BKI-1708 binders had lower abundancies in *T. gondii* ME49 tachyzoites treated with 2.5 µM BKI-1708 [24]: i) two hypothetical proteins (TGME49_313270, TGME49_205320); ii) a cold-shock DNA-binding domain-containing protein (TGME49_320600); iii) a putative eukaryotic translation initiation factor 3 subunit G (TGME49_294670) that specifically targets and initiates translation of a subset of mRNAs involved in cell proliferation; and iv) a zinc finger (CCCH-type) motif-containing protein (ME49_309200). Notably, the latter was detected in untreated tachyzoites, but absent in BKI-1708-treated parasites. CCCH-type zinc fingers are well known to bind RNA rather than DNA and play key roles in RNA processing, stability, and translation regulation, thereby contributing to post-transcriptional control of gene expression [43]. The downregulation or loss of these proteins in baryzoites suggests that they may represent direct binding targets of the compound, or alternatively components of protein complexes disrupted by its presence. Such changes could be either a direct consequence of compound binding — through mechanisms such as protein degradation or transcriptional repression — or an indirect result of a shutdown of associated pathways. Collectively, these perturbations may trigger inappropriate differentiation, slow parasite growth, and compromise developmental progression. Another finding was that the hypothetical protein TGME49_201860 was found to be the most highly abundant protein binding to both, quinine and BKI-1708 (Table 2), while its expression was downregulated in *T. gondii* baryzoites [24].

The results obtained in HFF showed that both, the compound (BKI-1708 and quinine) and the HFF infection status, had an influence on the protein composition of respective pull-down fractions. Nevertheless, a small set of nine general binding proteins was identified binding to both, BKI-1708 and quinine, regardless of the infection status. This set included RNA-binding proteins, as well as proteins involved in cytoskeletal organization, intracellular transport, and redox homeostasis. The overlap between the two affinity proteomes of BKI-1708 and quinine reflects again a shared affinity for the 5-amido-caboxamide core structure. In addition to these shared interactions, BKI-1708 also displayed compound-specific binding: twenty host proteins were uniquely detected in pull-downs from extracts of non-infected HFF, and eight additional host proteins interacted exclusively with BKI-1708 in extracts from *T. gondii*-infected cells.

Out of the total of twenty proteins found interacting exclusively with BKI-1708 in non-infected HFF, the two most abundant proteins were translation machinery-associated protein 7 (TMA7) with evolutionary links to translation in fungi and predicted functions in protein synthesis in humans; followed by Stathmin (STMN1), a microtubule-destabilizing protein [44,45]. Additionally, several other proteins involved in cytoskeletal regulation and intracellular trafficking were found to bind specifically to BKI-1708, including i) PDZ and LIM domain protein 1 (PDLIM1), which acts as a scaffold linking actin filaments to signaling pathways [46]; ii) isoform 2 of dihydropyrimidinase-related protein 2 (DPYSL2), necessary for signaling and subsequent remodeling of the cytoskeleton [47]; iii) isoform 10 of protein transport protein Sec31A (Sec31A), which promotes vesicle formation from the endoplasmic reticulum [48]; iv) SLAIN motif-containing protein 2 (SLAIN2), that regulates microtubule growth in interphase [49]; and v) microtubule-associated proteins 4 (MAP4) and 2 (MAP2), both involved in microtubule assembly and stabilization [50,51]. Annexins A11 and A7 (ANXA11, ANXA7) were also identified as BKI-1708 specific binders with reported functions

 doi:10.20944/preprints202604.0997.v1

associated with membranes dynamics and the cytoskeleton [52]. More recently, annexins have been implicated in RNA binding, although the mechanisms underlying this function remain unclear [53]. Other specific BKI-1708 binders directly involved in RNA-related processes include RNA-binding CCHC-type zinc finger nucleic acid binding protein (CNBP) [54] and eukaryotic translation initiation factor 4 gamma 2 (eIF4G2) [55]. Furthermore, two proteins with DNA-binding functions were identified in the BKI-1708-specific affino-proteome dataset: WD repeat-containing protein 5 (WDR5), a multifunctional protein with described role in histone modification [56]; and protein SET (SET), a multitasking factor that participates in transcription, apoptosis, nucleosome assembly, and histone chaperoning [57,58]. The third most abundant identified protein was secreted Ly-6/uPAR-related protein 1 (SLURP1) reportedly having antitumor activity [59]. In addition, CREB-regulated transcription coactivator 3 (CRTC3), a transcriptional coactivator that associates with CREB1 was identified as BKI-1708 binding protein. CRTC3 acts as a coactivator that enhances CREB's transcriptional activity in response to cellular signals such as stress or metabolic changes [60,61]. Lastly, Catalase (CAT) that catalyzes the degradation of hydrogen peroxide, thus protecting cells from its toxic effects [62] was found interacting with BKI-1708. Notably, *T. gondii* peroxiredoxin PRX3 with similar antioxidant functions was found to bind specifically to BKI-1708, with the highest rAbu of the set. In addition, and similarly with what was found in the host cells, the second most abundant protein in this set – the transport protein Sec31 - was also engaged by the compound in *T. gondii*, indicating the presence of shared molecular targets in parasites and host cells (Tables 1 and 4).

Overall, BKI-1708-binding proteins in *T. gondii* and non-infected HFF seem to be associated with largely similar pathways. This mirrors earlier findings on comparative DAC-MS using a closely related compound, BKI-1748, identifying respective binding proteins in *N. caninum* tachyzoite and zebrafish extracts [27]. In both organisms, a majority of BKI-1748 binding proteins was involved in RNA binding and modification, in particular, splicing, and eluates from both organisms contained proteins involved in DNA binding or modification and key steps of intermediate metabolism. However, while BKI-1748 DAC-MS of *Neospora* resulted in the identification of NcCDPK1 [27], one of the validated BKI-targets, as a drug-binding protein, neither TgCDPK1 nor TgMAPKL1 were identified as drug binders in this study. This could be because these proteins might interact with the drug only transiently, or binding conditions were suboptimal leading to instable interactions, or due to lack of sensitivity of the method if these proteins are present only at low concentrations. In any case, both BKI-1748 interacted with not only specific targets in apicomplexans, such as CDPK1, but also with targets in other eukaryotes, which are involved in common, essential pathways [27], and the same appears true for BKI-1708.

Infected cells had markedly less readouts overall which may reflect limitations related to sample availability due to cell lysis upon *T. gondii* infection. In addition, infected cells may undergo necrosis or apoptosis, allowing for the identification of associated proteins. Detection of a protein linked to apoptosis suggests that these effects represent infection-driven cellular responses rather than direct consequences of BKI-1708 treatment. In summary, eight proteins were found to interact exclusively with BKI-1708 in *T. gondii*-infected HFF, eleven proteins were specifically bound to quinine, and ten were identified in both BKI-1708 and quinine column eluates.

In contrast to non-infected HFF, with BKI-1708 binders involved in maintaining or remodeling the cytoskeleton, regulation of microtubules and actin filaments, RNA, DNA and protein-binding, specific BKI-1708 binders in *T. gondii*-infected cells were not primarily associated with cytoskeleton and intracellular transport functions. Instead, the detected proteins were mostly DNA and RNA-binders. Amongst these proteins, the most abundant was the secreted protein-binding extracellular glycoprotein lacritin (LACRT). LACRT, typically associated with lacrimal and salivary tissues, plays a role in immune regulation and tear secretion [63]. This may reflect a stress-induced expression or stabilization of LACRT, enabling it to interact with the compound despite its low basal expression in fibroblasts. The second most abundant protein was isoform 2 of polyglutamine-binding protein 1 (PQBP1-2). PQBP1 is a highly conserved intrinsically disordered scaffold protein involved in pre-mRNA splicing, transcriptional regulation, innate immunity, and neuronal development [64],

 doi:10.20944/preprints202604.0997.v1

mediating diverse cellular processes through its interaction with polyglutamine tracts [65]. Beyond these, the proteins binding exclusively to BKI-1708 in infected cells were associated with nucleic acid and protein metabolism, with only a single protein linked to energy metabolism. The mitochondrial L-lactate dehydrogenase B chain (LDHB) was the metabolic enzyme identified, associated with catalyzing the stereospecific interconversion of pyruvate and lactate coupled to the NADH/NAD^+ redox system [66]. Two nuclear proteins were also detected: isoform 2 of nuclear pore complex protein Nup153 (NUP153), a core component of the nuclear pore complex required for nucleocytoplasmic transport (Hase and Cordes, 2003), and isoform 2 of pescadillo homolog (PES1), a PeBoW complex member essential for rRNA processing and 60S ribosome biogenesis [67,68]. Other pulled-down proteins with RNA-binding activities include i) Isoform 2 of Myb-binding protein 1A (MYBBP1A), with a reported role in RNA biogenesis through interactions with the chromatin-associated factor PWP1 [69], and ii) Isoform 2 of proliferation marker protein Ki-67 (MKI67) [70]. Lastly, isoform 2 of suprabasin (SBSN) was identified, although its functional role remains unclear.

Overall, functions associated with the cytoskeleton, intracellular signaling and transport are absent in the BKI-1708 affino-proteome of *T. gondii*-infected HFF, possibly reflecting that infection modulates host signaling and chromatin-related pathways. It is known that *T. gondii* profoundly reprograms the host proteome and metabolism, with metabolic rewiring for parasite benefit, immune signaling modulation, and structural/cellular adjustments to support intracellular survival [71,72]. Host cytoskeletal regulators and actin dynamics are essential for *T. gondii* invasion and intracellular growth [73], making the host trafficking machinery and actin/microtubule-associated proteins critical for parasite establishment and survival. These infection-induced changes alter the accessibility of host proteins, which likely explains why BKI-1708 engages cytoskeletal targets in non-infected but not in infected host cells, while RNA-binding proteins remain engaged regardless of infection status.

A core set of twelve proteins were bound specifically to BKI-1708 in both *T. gondii* -infected and non-infected HFF. Proteins captured by BKI-1708 in both conditions were mostly involved in RNA binding, or were not annotated and thus designated as hypothetical proteins. Some of the proteins are functionally involved in stress-related pathways. One of the most abundant proteins identified was isoform 2 of splicing factor 1 (SF1), which is reported to bind to RNA and function in the early stages of pre-mRNA splicing [74,75]. In a previous study investigating the molecular targets of BKI-1748 using DAC-MS in *C. parvum* and host cells, isoform 2 of SF1 was also found to bind to both BKI-1748 and quinine in the human colon tumor cell line HCT-8 [28]. In the present study, isoform 2 of SF1 was identified in HFF as a specific binder of BKI-1708 but not of quinine, suggesting a potentially unique role for SF1 in the mechanism of action of BKI-1708. The compound may have a chemical structure or binding mode that allows it to selectively engage SF1, in contrast to BKI-1748. Alternatively, differences between host cell lines — such as SF1 expression levels, post-translational modifications, interacting partners, or subcellular localization — could influence the ability of SF1 to interact with BKI-1708 or quinine.

It is important to point out that proteins recovered from DAC-MS experiments may represent: i) direct binders present as intact, functional proteins; ii) proteins rendered accessible through cell lysis, including those from disrupted host or parasite compartments or degraded material; and iii) nonspecific, high-abundance or “sticky” contaminants. Moreover, DAC-MS has some intrinsic limitations, in that direct binding of a protein to a drug does not inherently demonstrate functional inhibition by the drug or that binding also occurs under native conditions or *in vivo*. For instance, the presence of EDTA in a protease inhibitor cocktail included in the lysis buffer could influence calcium-dependent interactions as for CDPK1 but also other proteins. Evidently, the fact that HFF do not exhibit any obvious impairment in viability upon exposure to BKI-1708 suggests that they have, in addition to the above possibilities, evolved mechanisms to circumvent potential adverse effects, at least at the concentrations used in this study. Lastly, kinase targets may be underrepresented depending on immobilization chemistry and active-site accessibility [25].

Despite these intrinsic methodological limitations, our results suggest that in *T. gondii* BKI-1708 has a broader impact beyond canonical kinase targets, including i) engagement of secretory

 doi:10.20944/preprints202604.0997.v1

organelles (ROP25, TgGRA29, TgGRA62, and micronemal TgPLP1); ii) binding to components of vesicular trafficking machinery (TgSEC13/23/31); iii) interaction with transcriptional/epigenetic control elements (TgAP2VIII-2, CHD1/SWI2/SNF2, PLU-1); iv) redox regulation (TgPRX3, TgTLAP4); and v) cytoskeleton-associated proteins (TgIMC25). This binding profile suggests that BKI-1708 perturbs protein trafficking, organelle biogenesis, stress homeostasis, and gene expression networks simultaneously. Collectively, these multilayered disruptions provide a mechanistic basis for defective cytokinesis, organelle segregation failure, and the emergence of multinucleated baryzoites under drug pressure. Consistent with this, as mentioned, BKI-1708- treated tachyzoites failed to complete normal division and egress. It is conceivable that this phenotype results from multi-target interactions, including RNA binding and modulation of cell cycle–related proteins, disrupting coordinated processes required for parasite replication and egress. Figure 5 schematically summarizes plausible drug-disrupted pathways based on BKI-engaged proteins, leading to the observed baryzoite phenotype under BKI-1708 treatment. The findings that BKI-1708 interacts potentially with multiple protein targets, align with the emerging view that antiprotozoal drugs often operate via multiple mechanisms rather than through a single, well-defined target [25].

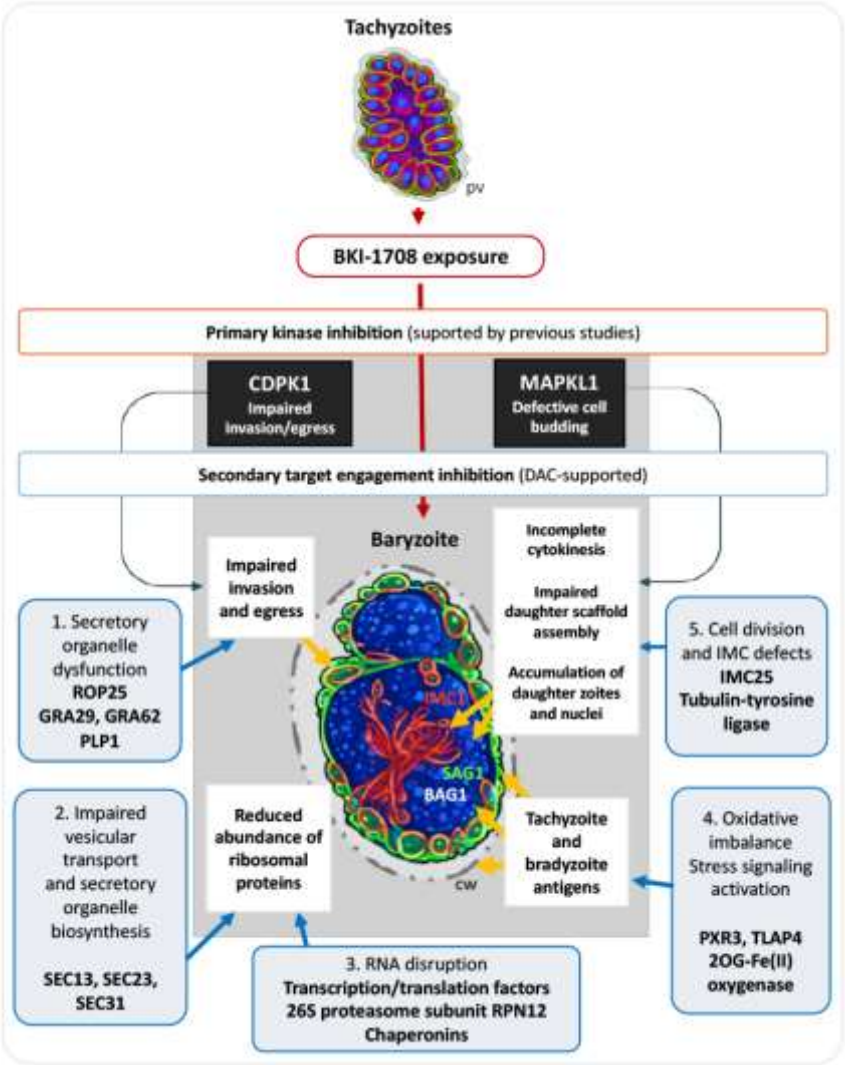

Figure 5. Schematic representation of proposed BKI-1708–mediated multi-layered disruption of *Toxoplasma gondii* tachyzoites leading to baryzoite formation. Tachyzoites situated within a parasitophorous vacuole (pv) are exposed to BKI-1708. The resulting aberrant baryzoites display mixed stage identity, co-expressing the tachyzoite marker surface antigen SAG1 and the bradyzoite antigen BAG1, with altered IMC organization and peripheral deposition of cyst wall-like material (cw).

 doi:10.20944/preprints202604.0997.v1

5. Conclusions

In *T. gondii* and in non-infected HFF, the molecular targets of BKI-1708 include proteins involved in RNA regulation, cytoskeleton dynamics, and intracellular transport. Infection of HFF reshapes the host protein binding profile, limiting the interaction with cytoskeletal proteins — since these targets are not as readily accessible in infected cells — while RNA-binding proteins remain consistently engaged regardless of infection status. In non-infected HFF and *T. gondii* tachyzoites, cytoskeletal and RNA-binding proteins represent core molecular targets of its activity. In *T. gondii*, engagement also extends to additional proteins involved in egress and invasion. Together, these findings provide a mechanistic explanation for the impaired cytokinesis phenotype observed in baryzoites induced by BKI treatment, and points towards a multifactorial mode of action of BKI-1708.

Supplementary Materials: The following supporting information can be downloaded at the website of this paper posted on Preprints.org, Table S1: HFF-binding proteins; Table S2: *Toxoplasma* binding proteins; Table S3: Functional categorization of binding proteins; supplementary Figure S1: Protein intensity distributions (PIDs) represented by boxplots of the log2-transformed IBAQ (intensity based absolute quantification); Supplementary Figure S2: Hierarchical clustering of the log2-transformed IBAQ intensities.

Author Contributions: For research articles with several authors, a short paragraph specifying their individual contributions must be provided. The following statements should be used "Conceptualization, J.M., M.F. and A.H.; methodology, M.F., J.M., M.H., S.B., A.C.U. and A.H.; software, M.H., A-C.U., and S.B.; validation, J.M. and M.F.; formal analysis, J.M. and M.F.; investigation, M.F., J.M., and A.H.; resources, A.H., K.K.O. and W.C.V.V.; data curation, M.F. and J.M.; writing—original draft preparation, M.F.; writing—review and editing, J.M., A.H., M.H., A-C.U., S.B., K.K.O. and W.C.V.V. visualization, A.H. and M.F.; supervision, A.H. and J.M.; project administration, A.H. and J.M.; funding acquisition, A.H., and W.C.V.V. All authors have read and agreed to the published version of the manuscript.

Funding: This research was funded by Swiss National Science Foundation, grant 310030_214897, the National Institutes of Health (NIH) grant R01HD102487 and R01AI55412, the Uniscientia Foundation, and a Swiss Government Excellence Fellowship awarded to M.F.

Institutional Review Board Statement: not applicable.

Data Availability Statement: The original contributions presented in this study are included in the article / Supplementary Materials. Further inquiries can be directed to the corresponding authors.

Conflicts of Interest: WCVV is an owner/officer of ParaTheraTech Inc, a company which is seeking to bring bumped kinase inhibitors to the animal health market. The funders of this study had no role in the design of the study; in the collection, analyses, or interpretation of data; in the writing of the manuscript; or in the decision to publish the results.

References

1. Dubey, J.P. *Toxoplasmosis of Animals and Humans*; CRC Press, 2021; ISBN 978-1-000-43149-0.
2. Martorelli Di Genova, B.; Wilson, S.K.; Dubey, J.P.; Knoll, L.J. Intestinal Delta-6-Desaturase Activity Determines Host Range for Toxoplasma Sexual Reproduction. *PLoS Biol* **2019**, *17*, e3000364, doi:10.1371/journal.pbio.3000364.
3. Almeria, S.; Dubey, J.P. Foodborne Transmission of Toxoplasma Gondii Infection in the Last Decade. An Overview. *Res Vet Sci* **2021**, *135*, 371–385, doi:10.1016/j.rvsc.2020.10.019.
4. Holec-Gąsior, L.; Sołowińska, K. Detection of Toxoplasma Gondii Infection in Small Ruminants: Old Problems, and Current Solutions. *Animals* **2023**, *13*, undefined-undefined, doi:10.3390/ani13172696.
5. Sullivan, W.J.; Jeffers, V. Mechanisms of Toxoplasma Gondii Persistence and Latency. *FEMS Microbiol Rev* **2012**, *36*, 717–733, doi:10.1111/j.1574-6976.2011.00305.x.
6. Weiss, L.M.; Kim, K. THE DEVELOPMENT AND BIOLOGY OF BRADYZOITES OF TOXOPLASMA GONDII. *Front Biosci* **2000**, *5*, D391–D405.

 doi:10.20944/preprints202604.0997.v1

7. Montoya, J.; Liesenfeld, O. Toxoplasmosis. *The Lancet* **2004**, *363*, 1965–1976, doi:10.1016/S0140-6736(04)16412-X.
8. Walana, W.; Odai, S.A.; Tamomh, A.G. Prevalence, Risk Factors, Diagnosis and Outcomes of *TOxoplasma Gondii* Infection in Pregnancy: A Review. *Parasitology International* **2026**, *110*, 103143, doi:10.1016/j.parint.2025.103143.
9. Liu, S.; Cai, M.; Liu, Z.; Gao, W.; Li, J.; Li, Y.; Abudouxukuer, X.; Zhang, J. Comprehensive Insights into the Development of Antitoxoplasmosis Drugs: Current Advances, Obstacles, and Future Perspectives. *J. Med. Chem.* **2024**, *67*, 20740–20764, doi:10.1021/acs.jmedchem.4c01733.
10. Choi, R.; Hulverson, M.A.; Huang, W.; Vidadala, R.S.R.; Whitman, G.R.; Barrett, L.K.; Schaefer, D.A.; Betzer, D.P.; Riggs, M.W.; Doggett, J.S.; et al. Bumped Kinase Inhibitors as Therapy for Apicomplexan Parasitic Diseases: Lessons Learned. *International Journal for Parasitology* **2020**, *50*, 413–422.
11. Huang, W.; Hulverson, M.A.; Choi, R.; Arnold, S.L.M.; Zhang, Z.; McCloskey, M.C.; Whitman, G.R.; Hackman, R.C.; Rivas, K.L.; Barrett, L.K.; et al. Development of 5-Aminopyrazole-4-Carboxamide-Based Bumped-Kinase Inhibitors for Cryptosporidiosis Therapy. *J. Med. Chem.* **2019**, *62*, 3135–3146.
12. Imhof, D.; Anghel, N.; Winzer, P.; Balmer, V.; Ramseier, J.; Hänggeli, K.; Choi, R.; Hulverson, M.; Whitman, G.; Arnold, S.; et al. In Vitro Activity, Safety and in Vivo Efficacy of the Novel Bumped Kinase Inhibitor BKI-1748 in Non-Pregnant and Pregnant Mice Experimentally Infected with Neospora Caninum Tachyzoites and Toxoplasma Gondii Oocysts. *International Journal for Parasitology: Drugs and Drug Resistance* **2021**, *16*.
13. Lourido, S.; Jeschke, G.R.; Turk, B.E.; Sibley, L.D. Exploiting the Unique ATP-Binding Pocket of Toxoplasma Calcium-Dependent Protein Kinase 1 to Identify Its Substrates. *ACS Chem Biol* **2013**, *8*, 1155–1162.
14. Jacot, D.; Soldati-Favre, D. Does Protein Phosphorylation Govern Host Cell Entry and Egress by the Apicomplexa? *Int J Med Microbiol* **2012**, *302*, 195–202.
15. Lourido, S.; Shuman, J.; Zhang, C.; Shokat, K.M.; Hui, R.; Sibley, L.D. Calcium-Dependent Protein Kinase 1 Is an Essential Regulator of Exocytosis in Toxoplasma. *Nature* **2010**, *465*, 359–362, doi:10.1038/nature09022.
16. Wei, F.; Wang, W.; Liu, Q. Protein Kinases of Toxoplasma Gondii: Functions and Drug Targets. *Parasitol Res* **2013**, *112*, 2121–2129.
17. Montgomery, J.A.; Alday, P.H.; Choi, R.; Khim, M.; Staker, B.L.; Hulverson, M.A.; Ojo, K.K.; Fan, E.; Van Voorhis, W.C.; Doggett, J.S. Bumped Kinase Inhibitors Inhibit Both Toxoplasma Gondii MAPKL1 and CDPK1. *ACS Infect. Dis.* **2025**, doi:10.1021/acsinfecdis.5c00051.
18. Sugi, T.; Kawazu, S.; Horimoto, T.; Kato, K. A Single Mutation in the Gatekeeper Residue in TgMAPKL-1 Restores the Inhibitory Effect of a Bumped Kinase Inhibitor on the Cell Cycle. *Int J Parasitol Drugs Drug Resist* **2014**, *5*, 1–8, doi:10.1016/j.ijpddr.2014.12.001.
19. Winzer, P.; Müller, J.; Aguado-Martínez, A.; Rahman, M.; Balmer, V.; Manser, V.; Ortega-Mora, L.M.; Ojo, K.K.; Fan, E.; Maly, D.J.; et al. In Vitro and In Vivo Effects of the Bumped Kinase Inhibitor 1294 in the Related Cyst-Forming Apicomplexans Toxoplasma Gondii and Neospora Caninum. *Antimicrob Agents Chemother* **2015**, *59*, 6361–6374, doi:10.1128/AAC.01236-15.
20. Winzer, P.; Anghel, N.; Imhof, D.; Balmer, V.; Ortega-Mora, L.-M.; Ojo, K.K.; Van Voorhis, W.C.; Müller, J.; Hemphill, A. Neospora Caninum: Structure and Fate of Multinucleated Complexes Induced by the Bumped Kinase Inhibitor BKI-1294. *Pathogens* **2020**, *9*, 382.
21. Winzer, P.; Müller, J.; Imhof, D.; Ritler, D.; Uldry, A.-C.; Braga-Lagache, S.; Heller, M.; Ojo, K.K.; Van Voorhis, W.C.; Ortega-Mora, L.-M.; et al. Neospora Caninum: Differential Proteome of Multinucleated Complexes Induced by the Bumped Kinase Inhibitor BKI-1294. *Microorganisms* **2020**, *8*, 801, doi:10.3390/microorganisms8060801.
22. de Sousa, M.C.F.; Imhof, D.; Hänggeli, K.P.A.; Choi, R.; Hulverson, M.A.; Arnold, S.L.M.; Van Voorhis, W.C.; Fan, E.; Roberto, S.-S.; Ortega-Mora, L.M.; et al. Efficacy of the Bumped Kinase Inhibitor BKI-1708 against the Cyst-Forming Apicomplexan Parasites Toxoplasma Gondii and Neospora Caninum in Vitro and in Experimentally Infected Mice. *Int J Parasitol Drugs Drug Resist* **2024**, *25*, 100553, doi:10.1016/j.ijpddr.2024.100553.

 doi:10.20944/preprints202604.0997.v1

23. Choi, R.; Hulverson, M.A.; Schaefer, D.A.; Betzer, D.P.; Riggs, M.W.; Huang, W.; Sun, V.; Whitman, G.R.; McCloskey, M.C.; Marsh, K.; et al. Anti-Cryptosporidium Efficacy of BKI-1708, an Inhibitor of Cryptosporidium Calcium-Dependent Protein Kinase 1. *PLOS Neglected Tropical Diseases* **2025**, *19*, e0013263, doi:10.1371/journal.pntd.0013263.
24. de Sousa, M.C.F.; Müller, J.; Hänggeli, K.P.A.; Heller, M.; Uldry, A.-C.; Braga-Lagache, S.; Leitao, A.; Ortega-Mora, L.-M.; Ojo, K.K.; Van Voorhis, W.C.; et al. Bumped Kinase Inhibitor BKI-1708 Interferes in Cytokinesis and Drives Baryzoite Conversion in the Cyst-Forming Apicomplexan Parasites Toxoplasma Gondii, Neospora Caninum and Besnoitia Besnoiti. *International Journal of Molecular Sciences* **2026**, *27*, 2914, doi:10.3390/ijms27062914.
25. Müller, J.; Boubaker, G.; Müller, N.; Uldry, A.-C.; Braga-Lagache, S.; Heller, M.; Hemphill, A. Investigating Antiprotozoal Chemotherapies with Novel Proteomic Tools—Chances and Limitations: A Critical Review. *International Journal of Molecular Sciences* **2024**, *25*, 6903, doi:10.3390/ijms25136903.
26. Liles, N.W.; Page, E.E.; Liles, A.L.; Vesely, S.K.; Raskob, G.E.; George, J.N. Diversity and Severity of Adverse Reactions to Quinine: A Systematic Review. *Am J Hematol* **2016**, *91*, 461–466, doi:10.1002/ajh.24314.
27. Müller, J.; Anghel, N.; Imhof, D.; Hänggeli, K.; Uldry, A.-C.; Braga-Lagache, S.; Heller, M.; Ojo, K.K.; Ortega-Mora, L.-M.; Van Voorhis, W.C.; et al. Common Molecular Targets of a Quinolone Based Bumped Kinase Inhibitor in Neospora Caninum and Danio Rerio. *Int J Mol Sci* **2022**, *23*, 2381.
28. Ajiboye, J.; Uldry, A.-C.; Heller, M.; Naguleswaran, A.; Fan, E.; Van Voorhis, W.C.; Hemphill, A.; Müller, J. Molecular Targets of the 5-Amido-Carboxamide Bumped Kinase Inhibitor BKI-1748 in Cryptosporidium Parvum and HCT-8 Host Cells. *International Journal of Molecular Sciences* **2024**, *25*, 2707, doi:10.3390/ijms25052707.
29. Müller, J.; Schlange, C.; Heller, M.; Uldry, A.-C.; Braga-Lagache, S.; Haynes, R.K.; Hemphill, A. Proteomic Characterization of Toxoplasma Gondii ME49 Derived Strains Resistant to the Artemisinin Derivatives Artemiside and Artemisone Implies Potential Mode of Action Independent of ROS Formation. *International Journal for Parasitology: Drugs and Drug Resistance* **2023**, *21*, 1–12.
30. Semeraro, M.; Boubaker, G.; Scaccaglia, M.; Müller, J.; Vigneswaran, A.; Hänggeli, K.P.A.; Amdouni, Y.; Kramer, L.H.; Vismarra, A.; Genchi, M.; et al. Transient Adaptation of Toxoplasma Gondii to Exposure by Thiosemicarbazone Drugs That Target Ribosomal Proteins Is Associated with the Upregulated Expression of Tachyzoite Transmembrane Proteins and Transporters. *Int J Mol Sci* **2024**, *25*, 9067, doi:10.3390/ijms25169067.
31. Kong, A.T.; Leprevost, F.V.; Avtonomov, D.M.; Mellacheruvu, D.; Nesvizhskii, A.I. MSFragger: Ultrafast and Comprehensive Peptide Identification in Mass Spectrometry–Based Proteomics. *Nat Methods* **2017**, *14*, 513–520, doi:10.1038/nmeth.4256.
32. Schwanhäusser, B.; Busse, D.; Li, N.; Dittmar, G.; Schuchhardt, J.; Wolf, J.; Chen, W.; Selbach, M. Global Quantification of Mammalian Gene Expression Control. *Nature* **2011**, *473*, 337–342, doi:10.1038/nature10098.
33. Fereig, R.M.; Nishikawa, Y. Genetic Disruption of Toxoplasma Gondii Peroxiredoxin (TgPrx) 1 and 3 Reveals the Essential Role of TgPrx3 in Protecting Mice from Fatal Consequences of Toxoplasmosis. *Int J Mol Sci* **2022**, *23*, 3076, doi:10.3390/ijms23063076.
34. Tang, B.L.; Peter, F.; Krijnse-Locker, J.; Low, S.H.; Griffiths, G.; Hong, W. The Mammalian Homolog of Yeast Sec13p Is Enriched in the Intermediate Compartment and Is Essential for Protein Transport from the Endoplasmic Reticulum to the Golgi Apparatus. *Mol Cell Biol* **1997**, *17*, 256–266, doi:10.1128/MCB.17.1.256.
35. Zhang, X.; Zhang, T.; Liu, J.; Li, M.; Fu, Y.; Xu, J.; Liu, Q. Functional Characterization of a Unique Cytochrome P450 in Toxoplasma Gondii. *Oncotarget* **2017**, *8*, 115079–115088, doi:10.18632/oncotarget.23023.
36. Marshall, E.S.; Elshekiha, H.M.; Hakimi, M.-A.; Flynn, R.J. Toxoplasma Gondii Peroxiredoxin Promotes Altered Macrophage Function, Caspase-1-Dependent IL-1β Secretion Enhances Parasite Replication. *Vet Res* **2011**, *42*, 80, doi:10.1186/1297-9716-42-80.
37. Bosch, S.S.; Kronenberger, T.; Meissner, K.A.; Zimbres, F.M.; Stegehake, D.; Izui, N.M.; Schettert, I.; Liebau, E.; Wrenger, C. Oxidative Stress Control by Apicomplexan Parasites. *BioMed Research International* **2015**, *2015*, 351289, doi:10.1155/2015/351289.

 doi:10.20944/preprints202604.0997.v1

38. Kafsack, B.F.C.; Pena, J.D.O.; Coppens, I.; Ravindran, S.; Boothroyd, J.C.; Carruthers, V.B. Rapid Membrane Disruption by a Perforin-like Protein Facilitates Parasite Exit from Host Cells. *Science* **2009**, *323*, 530–533, doi:10.1126/science.1165740.
39. Li, M.; Wang, H.; Liu, J.; Hao, P.; Ma, L.; Liu, Q. The Apoptotic Role of Metacaspase in Toxoplasma Gondii. *Front Microbiol* **2015**, *6*, 1560, doi:10.3389/fmicb.2015.01560.
40. Li, M.; Liu, J.; Wu, Y.; Wu, Y.; Sun, X.; Fu, Y.; Zhang, X.; Liu, Q. Requirement of Toxoplasma Gondii Metacaspases for IMC1 Maturation, Endodyogeny and Virulence in Mice. *Parasites & Vectors* **2021**, *14*, doi:10.1186/s13071-021-04878-0.
41. Radke, J.B.; Worth, D.; Hong, D.; Huang, S.; Jr, W.J.S.; Wilson, E.H.; White, M.W. Transcriptional Repression by ApiAP2 Factors Is Central to Chronic Toxoplasmosis. *PLOS Pathogens* **2018**, *14*, e1007035, doi:10.1371/journal.ppat.1007035.
42. Pachano, B.; Farhat, D.C.; Shahinas, M.; Von Velsen, J.; Corrao, C.; Belmudes, L.; De Bock, P.-J.; Mas, C.; Couté, Y.; Bowler, M.W.; et al. An ISWI-Related Chromatin Remodeller Regulates Stage-Specific Gene Expression in Toxoplasma Gondii. *Nat Microbiol* **2025**, *10*, 1156–1170, doi:10.1038/s41564-025-01980-2.
43. Hurt, J.A.; Obar, R.A.; Zhai, B.; Farny, N.G.; Gygi, S.P.; Silver, P.A. A Conserved CCCH-Type Zinc Finger Protein Regulates mRNA Nuclear Adenylation and Export. *J Cell Biol* **2009**, *185*, 265–277, doi:10.1083/jcb.200811072.
44. Howell, B.; Larsson, N.; Gullberg, M.; Cassimeris, L. Dissociation of the Tubulin-Sequestering and Microtubule Catastrophe-Promoting Activities of Oncoprotein 18/Stathmin. *Mol Biol Cell* **1999**, *10*, 105–118, doi:10.1091/mbc.10.1.105.
45. Sobel, A.; Boutterin, M.C.; Beretta, L.; Chneiweiss, H.; Doye, V.; Peyro-Saint-Paul, H. Intracellular Substrates for Extracellular Signaling. Characterization of a Ubiquitous, Neuron-Enriched Phosphoprotein (Stathmin). *J Biol Chem* **1989**, *264*, 3765–3772.
46. Kotaka, M.; Kostin, S.; Ngai, S.; Chan, K.; Lau, Y.; Lee, S.M.; Li, H. y; Ng, E.K.; Schaper, J.; Tsui, S.K.; et al. Interaction of hCLIM1, an Enigma Family Protein, with Alpha-Actinin 2. *J Cell Biochem* **2000**, *78*, 558–565, doi:10.1002/1097-4644(20000915)78:4%3C558::aid-jcb5%3E3.0.co;2-i.
47. Rahajeng, J.; Giridharan, S.S.P.; Naslavsky, N.; Caplan, S. Collapsin Response Mediator Protein-2 (Crmp2) Regulates Trafficking by Linking Endocytic Regulatory Proteins to Dynein Motors. *J Biol Chem* **2010**, *285*, 31918–31922, doi:10.1074/jbc.C110.166066.
48. Tang, B.L.; Zhang, T.; Low, D.Y.; Wong, E.T.; Horstmann, H.; Hong, W. Mammalian Homologues of Yeast Sec31p. An Ubiquitously Expressed Form Is Localized to Endoplasmic Reticulum (ER) Exit Sites and Is Essential for ER-Golgi Transport. *J Biol Chem* **2000**, *275*, 13597–13604, doi:10.1074/jbc.275.18.13597.
49. van der Vaart, B.; Manatschal, C.; Grigoriev, I.; Olieric, V.; Gouveia, S.M.; Bjelic, S.; Demmers, J.; Vorobjev, I.; Hoogenraad, C.C.; Steinmetz, M.O.; et al. SLAIN2 Links Microtubule plus End-Tracking Proteins and Controls Microtubule Growth in Interphase. *J Cell Biol* **2011**, *193*, 1083–1099, doi:10.1083/jcb.201012179.
50. Gong, C.X.; Wegiel, J.; Lidsky, T.; Zuck, L.; Avila, J.; Wisniewski, H.M.; Grundke-Iqbal, I.; Iqbal, K. Regulation of Phosphorylation of Neuronal Microtubule-Associated Proteins MAP1b and MAP2 by Protein Phosphatase-2A and -2B in Rat Brain. *Brain Res* **2000**, *853*, 299–309, doi:10.1016/s0006-8993(99)02294-5.
51. Wang, L.; Paudyal, S.C.; Kang, Y.; Owa, M.; Liang, F.-X.; Spektor, A.; Knaut, H.; Sánchez, I.; Dynlacht, B.D. Regulators of Tubulin Polyglutamylation Control Nuclear Shape and Cilium Disassembly by Balancing Microtubule and Actin Assembly. *Cell Res* **2022**, *32*, 190–209, doi:10.1038/s41422-021-00584-9.
52. Gerke, V.; Moss, S.E. Annexins: From Structure to Function. *Physiological Reviews* **2002**, *82*, 331–371, doi:10.1152/physrev.00030.2001.
53. Tartaglia, G.G.; Hollås, H.; Håvik, B.; Vedeler, A.; Pastore, A. The RNA-Binding Properties of Annexins. *J Mol Biol* **2025**, *437*, 168933, doi:10.1016/j.jmb.2024.168933.
54. Benhalevy, D.; Gupta, S.K.; Danan, C.H.; Ghosal, S.; Sun, H.-W.; Kazemier, H.G.; Paeschke, K.; Hafner, M.; Juranek, S.A. The Human CCHC-Type Zinc Finger Nucleic Acid-Binding Protein Binds G-Rich Elements in Target mRNA Coding Sequences and Promotes Translation. *Cell Rep* **2017**, *18*, 2979–2990, doi:10.1016/j.celrep.2017.02.080.

 doi:10.20944/preprints202604.0997.v1

55. Pyronnet, S.; Dostie, J.; Sonenberg, N. Suppression of Cap-Dependent Translation in Mitosis. *Genes Dev* **2001**, *15*, 2083–2093, doi:10.1101/gad.889201.
56. Couture, J.-F.; Collazo, E.; Trievel, R.C. Molecular Recognition of Histone H3 by the WD40 Protein WDR5. *Nat Struct Mol Biol* **2006**, *13*, 698–703, doi:10.1038/nsmb1116.
57. Beresford, P.J.; Zhang, D.; Oh, D.Y.; Fan, Z.; Greer, E.L.; Russo, M.L.; Jaju, M.; Lieberman, J. Granzyme A Activates an Endoplasmic Reticulum-Associated Caspase-Independent Nuclease to Induce Single-Stranded DNA Nicks. *J Biol Chem* **2001**, *276*, 43285–43293, doi:10.1074/jbc.M108137200.
58. Fan, Z.; Beresford, P.J.; Oh, D.Y.; Zhang, D.; Lieberman, J. Tumor Suppressor NM23-H1 Is a Granzyme A-Activated DNase during CTL-Mediated Apoptosis, and the Nucleosome Assembly Protein SET Is Its Inhibitor. *Cell* **2003**, *112*, 659–672, doi:10.1016/s0092-8674(03)00150-8.
59. Ridge, R.J.; Sloane, N.H. Partial N-Terminal Amino Acid Sequence of the Anti-Neoplastic Urinary Protein (ANUP) and the Anti-Tumour Effect of the N-Terminal Nonapeptide of the Unique Cytokine Present in Human Granulocytes. *Cytokine* **1996**, *8*, 1–5, doi:10.1006/cyto.1996.0001.
60. Iourgenko, V.; Zhang, W.; Mickanin, C.; Daly, I.; Jiang, C.; Hexham, J.M.; Orth, A.P.; Miraglia, L.; Meltzer, J.; Garza, D.; et al. Identification of a Family of cAMP Response Element-Binding Protein Coactivators by Genome-Scale Functional Analysis in Mammalian Cells. *Proc Natl Acad Sci U S A* **2003**, *100*, 12147–12152, doi:10.1073/pnas.1932773100.
61. Screaton, R.A.; Conkright, M.D.; Katoh, Y.; Best, J.L.; Canettieri, G.; Jeffries, S.; Guzman, E.; Niessen, S.; Yates, J.R.; Takemori, H.; et al. The CREB Coactivator TORC2 Functions as a Calcium- and cAMP-Sensitive Coincidence Detector. *Cell* **2004**, *119*, 61–74, doi:10.1016/j.cell.2004.09.015.
62. Takeuchi, A.; Miyamoto, T.; Yamaji, K.; Masuho, Y.; Hayashi, M.; Hayashi, H.; Onozaki, K. A Human Erythrocyte-Derived Growth-Promoting Factor with a Wide Target Cell Spectrum: Identification as Catalase. *Cancer Res* **1995**, *55*, 1586–1589.
63. Chang, V.; Mahoney, K.E.; Lian, I.; Chen, R.; Chung, N.; Utheim, T.P.; Karlsson, N.G.; Malaker, S.A. In-Depth Analysis of the Tear Fluid Glycoproteome Reveals Diverse Lacritin Glycosylation and Spliceoforms 2025, 2025.06.13.659589.
64. Wang, Q.; Moore, M.J.; Adelmant, G.; Marto, J.A.; Silver, P.A. PQBP1, a Factor Linked to Intellectual Disability, Affects Alternative Splicing Associated with Neurite Outgrowth. *Genes Dev* **2013**, *27*, 615–626, doi:10.1101/gad.212308.112.
65. Waragai, M.; Lammers, C.H.; Takeuchi, S.; Imafuku, I.; Udagawa, Y.; Kanazawa, I.; Kawabata, M.; Mouradian, M.M.; Okazawa, H. PQBP-1, a Novel Polyglutamine Tract-Binding Protein, Inhibits Transcription Activation by Brn-2 and Affects Cell Survival. *Hum Mol Genet* **1999**, *8*, 977–987, doi:10.1093/hmg/8.6.977.
66. Chen, Y.-J.; Mahieu, N.G.; Huang, X.; Singh, M.; Crawford, P.A.; Johnson, S.L.; Gross, R.W.; Schaefer, J.; Patti, G.J. Lactate Metabolism Is Associated with Mammalian Mitochondria. *Nat Chem Biol* **2016**, *12*, 937–943, doi:10.1038/nchembio.2172.
67. Hölzel, M.; Grimm, T.; Rohrmoser, M.; Malamoussi, A.; Harasim, T.; Gruber-Eber, A.; Kremmer, E.; Eick, D. The BRCT Domain of Mammalian Pes1 Is Crucial for Nucleolar Localization and rRNA Processing. *Nucleic Acids Res* **2007**, *35*, 789–800, doi:10.1093/nar/gkl1058.
68. Rohrmoser, M.; Hölzel, M.; Grimm, T.; Malamoussi, A.; Harasim, T.; Orban, M.; Pfisterer, I.; Gruber-Eber, A.; Kremmer, E.; Eick, D. Interdependence of Pes1, Bop1, and WDR12 Controls Nucleolar Localization and Assembly of the PeBoW Complex Required for Maturation of the 60S Ribosomal Subunit. *Mol Cell Biol* **2007**, *27*, 3682–3694, doi:10.1128/MCB.00172-07.
69. Liu, Y.; Mattila, J.; Ventelä, S.; Yadav, L.; Zhang, W.; Lamichane, N.; Sundström, J.; Kauko, O.; Grénman, R.; Varjosalo, M.; et al. PWP1 Mediates Nutrient-Dependent Growth Control through Nucleolar Regulation of Ribosomal Gene Expression. *Dev Cell* **2017**, *43*, 240-252.e5, doi:10.1016/j.devcel.2017.09.022.
70. Cuylen, S.; Blaukopf, C.; Politi, A.Z.; Müller-Reichert, T.; Neumann, B.; Poser, I.; Ellenberg, J.; Hyman, A.A.; Gerlich, D.W. Ki-67 Acts as a Biological Surfactant to Disperse Mitotic Chromosomes. *Nature* **2016**, *535*, 308–312, doi:10.1038/nature18610.
71. Blume, M.; Seeber, F. Metabolic Interactions between Toxoplasma Gondii and Its Host. *F1000Res* **2018**, *7*, F1000 Faculty Rev-1719, doi:10.12688/f1000research.16021.1.

 doi:10.20944/preprints202604.0997.v1

72. Sun, H.; Li, J.; Wang, L.; Yin, K.; Xu, C.; Liu, G.; Xiao, T.; Huang, B.; Wei, Q.; Gong, M.; et al. Comparative Proteomics Analysis for Elucidating the Interaction Between Host Cells and Toxoplasma Gondii. *Front Cell Infect Microbiol* **2021**, *11*, 643001, doi:10.3389/fcimb.2021.643001.
73. Wu, S.-Z.; Wei, H.-X.; Jiang, D.; Li, S.-M.; Zou, W.-H.; Peng, H.-J. Genome-Wide CRISPR Screen Identifies Host Factors Required by Toxoplasma Gondii Infection. *Front Cell Infect Microbiol* **2020**, *9*, 460, doi:10.3389/fcimb.2019.00460.
74. Arning, S.; Grüter, P.; Bilbe, G.; Krämer, A. Mammalian Splicing Factor SF1 Is Encoded by Variant cDNAs and Binds to RNA. *RNA* **1996**, *2*, 794–810.
75. Wang, X.; Bruderer, S.; Rafi, Z.; Xue, J.; Milburn, P.J.; Krämer, A.; Robinson, P.J. Phosphorylation of Splicing Factor SF1 on Ser20 by cGMP-Dependent Protein Kinase Regulates Spliceosome Assembly. *EMBO J* **1999**, *18*, 4549–4559, doi:10.1093/emboj/18.16.4549.